General model for the description of the third-order optical nonlinearities in conjugated systems: Application to the all-*trans* β-carotene molecule

D. Beljonne, J. Cornil, Z. Shuai, and J. L. Brédas
Service de Chimie des Matériaux Nouveaux, Centre de Recherche en Electronique et Photonique Moléculaires, Université de Mons-Hainaut, 7000 Mons, Belgium

F. Rohlfing and D. D. C. Bradley
Department of Physics, Centre for Molecular Materials, University of Sheffield, Sheffield S3 7RH, United Kingdom

W. E. Torruellas,* V. Ricci, and G. I. Stegeman
Center for Research and Education in Optics and Lasers (CREOL), University of Central Florida, Orlando, Florida 32826
(Received 10 April 1996; revised manuscript received 13 August 1996)

On the basis of an extended configuration-interaction description of the lowest singlet excited states, we investigate the third-order nonlinear optical response of the β-carotene molecule by means of the sum-over-states approach. We first uncover the nature of the electronic states contributing primarily to the cubic molecular polarizabilities. From this starting point, we apply a simplified model to evaluate the frequency-dependent third-harmonic generation (THG) and electroabsorption (EA) spectra; the vibronic structure of the spectra is described by taking into account Franck-Condon factors calculated in a displaced oscillator model. For both the THG and EA processes, we obtain good agreement between the theoretical simulations and the experimental data, which underlines the general character of our model. [S0163-1829(97)00603-6]

I. INTRODUCTION

Due to their highly delocalized π-electronic cloud, conjugated polymers and oligomers are usually characterized by very large optical nonlinearities, which make them suitable for a wide range of applications in the field of information technology.[1] In order to develop organic materials with improved nonlinear optical (NLO) properties, a good description of the microscopic origin of the NLO response is required.

In this context, because such compounds possess the largest nonlinearities, many experimental efforts have been devoted toward the characterization of the nonlinear response of conjugated *polymers*, such as polydiacetylene (PDA),[2–5] polyacetylene (PA),[6–8] or polythiophene (PT).[9–11] However, in this approach, one usually suffers from two important drawbacks: (i) The polymeric materials (except for the particular case of PDA) are generally formed by an inhomogeneous mixing of chains with different effective conjugation lengths, which makes the analysis of the optical properties somewhat uncertain; and (ii) the information provided by quantum-chemical models for infinite chains has to be considered with much care in view of the different approximations usually assumed.

Recently, another strategy has been developed, that consists of investigating the nonlinear susceptibilities of *well-defined oligomers*, such as the dimethyl-amino-nitro-stilbene (DANS) molecule[12,13] or β-carotene.[14–16] We consider β-carotene (Fig. 1) to be the molecule of choice as a prototype for the description of the nonlinearities in conjugated systems: with 11 double bonds, it can be considered as a good model for polyacetylene, while its finite size allows one to apply high-level theoretical techniques for the calculation of its NLO response.

The dispersion of the modulus of the third-order nonlinear susceptibility of a β-carotene-doped polystyrene film was extensively studied by van Beek and co-workers[15] via third-harmonic generation (THG) throughout the $1B_u$ absorption band (from 2.3 to 2.9 eV). These authors interpret the frequency-dependent THG curve on the basis of a three-electronic-state model, taking into account six Franck-Condon active normal modes in the resonant electronic state. Such a three-state model (including the $1A_g$, $1B_u$, and mA_g states) is supported by quantum-chemical calculations on polyenes, indicating large transition dipole moments between the $1A_g$ and $1B_u$ states and between the $1B_u$ and mA_g states.[17–20] Although the three-state model of van Beek and co-workers provides an overall reliable description of the THG process in the resonant region, it misses the falloff of the cubic response to the blue of the $1B_u$ band. A slightly better agreement with the experimental data in this energy range is obtained by including in the sum-over-states (SOS) formalism another low-lying state, i.e., the two-photon $2A_g$ excited state.[14,21] The shape of the THG curve between $\sim$0.5 and $\sim$1.2 eV is then explained on the basis of a four-state model (including the $1A_g$, $2A_g$, $1B_u$, and mA_g states) and overlapping $2A_g$ and $1B_u$ resonances.[21]

Here we reinvestigate the nature of the essential states dominating the third-order response of β-carotene, and calculate the dispersion curves for the third-harmonic genera-

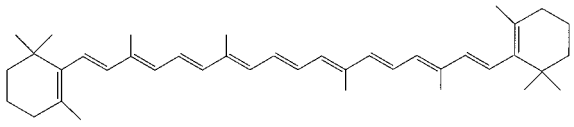

FIG. 1. Chemical structure of the β-carotene molecule.

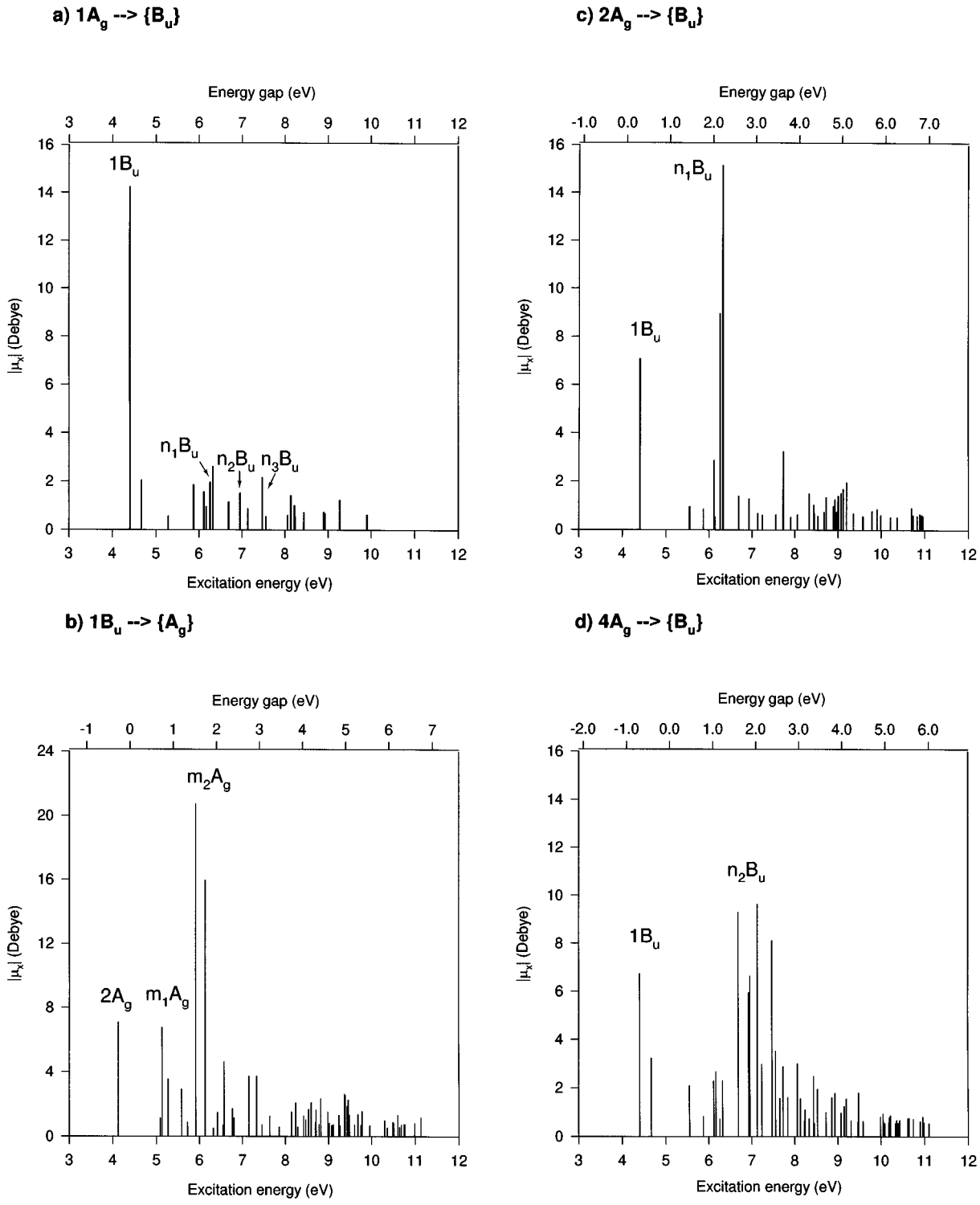

FIG. 2. INDO/MRD-CI transition dipole moments (in D) from (a) the ground state to the one-photon excited states; (b) the $1B_u$ state to A_g excited states; (c) the $2A_g$ state to B_u excited states; and (d), (e), and (f) the states forming the m_1A_g and m_2A_g bands to B_u excited states. The horizontal axis (lower abscissa) is the state energy with respect to the ground state; the upper abscissa gives the energy gaps.

tion (THG) and electroabsorption (EA) processes. By comparison to the body of knowledge accumulated so far, our contribution to the description of the third-order response of β-carotene should be regarded as relevant for the following reasons:

(i) The model proposed to describe the cubic nonlinearity is based on a *high-level description of the couplings* between the electronic states of β-carotene, obtained by considering the *full chemical structure* of the molecule.

(ii) The model is applied to simulate two third-order phenomena. More particularly, we extend the investigation of the THG process to higher fundamental excitation energies (up to 1.8 eV), for which recent experimental measurements have been performed,[22] and make use of the complementary

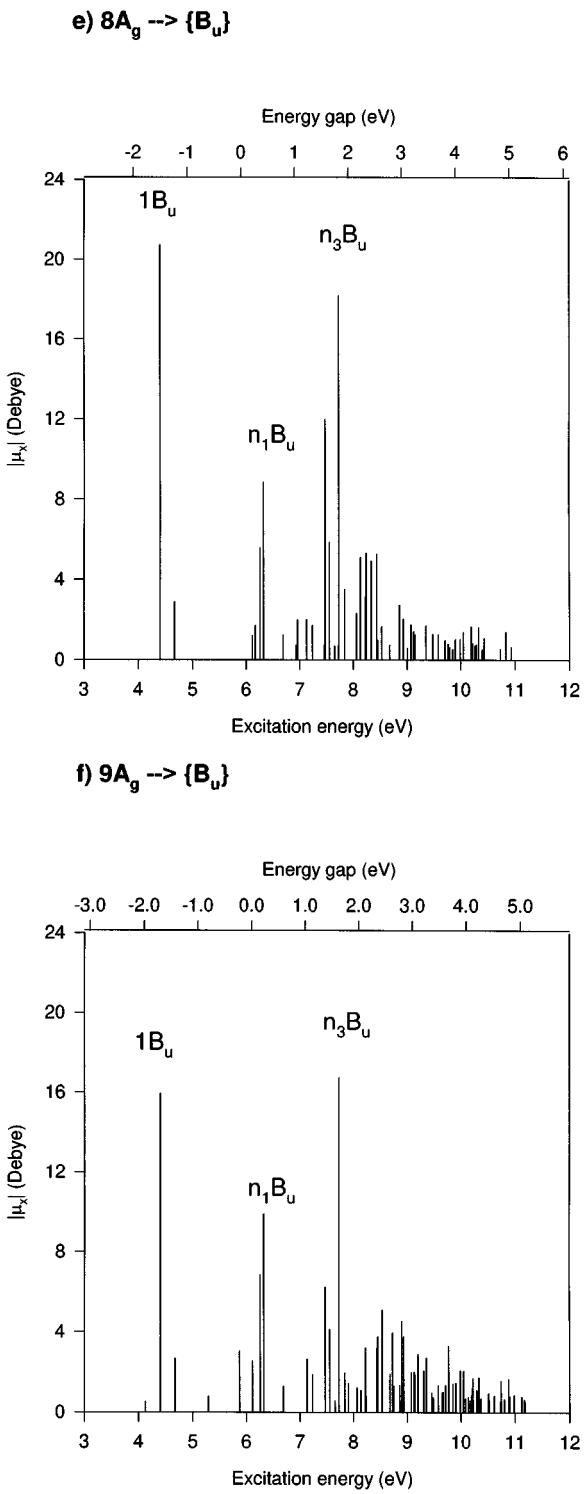

FIG. 2. (*Continued*).

information provided by the EA data.[16] We are thus confident in the *general character of the model* proposed.

II. EXPERIMENTAL DETAILS

The experimental data reported here were recorded for two different samples of β-carotene. The first one (hereafter denoted sample 1) was prepared in Sheffield by spincoating toluene solutions of β-carotene (10% by weight) and polystyrene onto spectrosil substrates on which 40 interdigitated aluminum electrodes with gaps of 100 μm were preevaporated. Sample 1 was used to measure the linear optical-absorption and electroabsorption spectra. Both EA and one-photon absorption spectra were recorded at liquid-nitrogen temperature to enhance the resolution of spectral features. The EA spectrometer consists of a light source, a monochromator, a cold finger liquid-nitrogen cryostat into which the sample is mounted, and a detector. Measurements involve monitoring the modulation in the transmission of the light through a sample in response to perturbation by an external electric field. The transmission T and change of transmission ΔT are simultaneously measured as a function of photon energy via a standard lock-in technique: The reference frequency for measurements of ΔT was the second harmonic of the modulation frequency (quadratic electro-optic response). The normalized EA signal is obtained by taking the ratio $-\Delta T/T$, which follows to good approximation $d\Delta\alpha$, the film thickness times the change in absorption coefficient. Additional details of the apparatus and analysis are given elsewhere.[16]

The third-harmonic generation spectrum of β-carotene has been recorded in Orlando; the sample (hereafter denoted sample 2) used for the measurements was prepared by depositing polystyrene thin films with β-carotene at a 4% molar content on top of fused silica substrates. The experimental setup has been described previously.[14] Briefly, an injection-seeded Q-switched Nd:YAG (yttrium aluminum garnet) laser was frequency doubled to pump a dye laser operated with DCM and Rhodamine-110 dyes. Maker fringes were recorded by focusing the vertically polarized near-infrared laser beam onto the sample placed in vacuum, with the film facing the photomultiplier. The optical-absorption spectrum of this sample was also measured for comparison.

III. ELECTRONIC MODEL

The ground-state geometry of the β-carotene molecule has been optimized at the AM1 (Austin Model 1) level.[23] The AM1 calculations indicate that the molecule is essentially planar. However, there are torsions around the external single bonds connecting the conjugated chain to the cyclohexene rings;[24] such a deviation from planarity is due to steric hindrance, and reduces the effective conjugation length of the molecule. In the conjugated segment, the single and double bonds are close to 1.45 and 1.35 Å, respectively, leading to an average bond-length alternation of $\sim$0.10 Å.

On the basis of the AM1-optimized geometry, we describe the excited states of β-carotene by means of the intermediate neglect of differential overlap (INDO) (Ref. 25) multireference double-configuration-interaction (MRD-CI) (Ref. 26) technique. The MRD-CI scheme has been described in detail elsewhere.[27] Briefly, it consists of a two-step selection of the electronic configurations, each step being based on a single and double configuration-interaction (SD-CI) calculation. Globally, single, double, triple, and quadruple excitations with respect to the Hartree-Fock reference determinants are included in the CI expansion of the multielectronic wave functions, at a cost largely inferior to that of a conventional quadruple excitation configuration-interaction

(QCI) calculation. Here, we have considered single and double excitations from the seven highest π to the seven lowest $\pi^\star$ molecular orbitals on the basis of the Hartree-Fock determinant, and from the five highest π and five lowest $\pi^\star$ levels on the basis of (i) the electronic configuration built by promoting one electron from the highest occupied molecular orbital (HOMO) to the lowest unoccupied molecular orbital (LUMO); (ii) the configuration resulting from the promotion of one electron from the HOMO to the LUMO+1; and (iii) the determinant where two electrons are excited from the HOMO to the LUMO. Even with such a sophisticated technique, the electronic correlation effects are not fully taken into account. Therefore, we have adopted the Mataga-Nishimoto potential[28] rather than the Ohno-Klopman potential[29] to describe the electron-electron interactions, since the former expression is characterized by a larger screening effect and, hence, implicitly introduces a larger part of electron correlation when the INDO method is coupled to the MRD-CI formalism.

In Fig. 2, we sketch the longitudinal transition dipole moments among the main electronic states of β-carotene, as calculated at the INDO/MRD-CI level. From Fig. 2, we can draw the following conclusions:

(i) The ground state $1A_g$ possesses an overwhelming transition dipole moment with the first one-photon allowed excited state, $1B_u$ [Fig. 2(a)].

(ii) The $1B_u$ state is itself coupled via large electronic transition moments to several A_g excited states, mainly the $2A_g$, $4A_g$, $8A_g$, and $9A_g$ states [Fig. 2(b)].

(iii) Each relevant two-photon state, that is coupled to the $1B_u$ excited state, also displays huge transition dipole moments with higher-lying B_u excited states; $2A_g$ with $8B_u$ and $9B_u$ states; $4A_g$ mainly with $10B_u$, $11B_u$, $12B_u$, and $13B_u$ states; and $8A_g$ and $9A_g$ with $8B_u$, $9B_u$, $15B_u$, and $18B_u$ states [Figs. 2(c)–2(f)].

It is worth stressing that in the case of the octatetraene molecule very similar coupling schemes have been obtained on the basis of both the INDO/MRD-CI description of the excited states and high-level *ab initio* CASSCF/CASPT2 calculations.[30] This confirms the overall reliability of the INDO/MRD-CI approach we use to characterize β-carotene.

TABLE I. Labeling of the ''bands'' formed by the main electronic excited states in the description of the third-order polarizability of β-carotene. We chose arbitrary letters (m_1, m_2, n_1, n_2, and n_3) to differentiate these bands (Ref. 36).

Band	Excited states
$2A_g$	$2A_g$
$1B_u$	$1B_u$
m_1A_g	$4A_g$
m_2A_g	$8A_g$,$9A_g$
n_1B_u	$8B_u$,$9B_u$
n_2B_u	$10B_u$,$11B_u$,$12B_u$,$13B_u$
n_3B_u	$15B_u$,$18B_u$

A closer look at Fig. 2 clearly shows the existence of ''bands'' of closely spaced excited states with a given symmetry that share oscillator strength with other bands belonging to the other representation. Therefore, in the following, we will refer to these bands rather than to the individual excited states and use the labels defined in Table I (note that the letters m_1, m_2, n_1, n_2, and n_3 in this table denote the quantum numbers of the different bands).

With this information as our starting point, we computed the third-order molecular polarizability γ by means of the sum-over-states (SOS) approach.[31] Considering a power expansion of the Stark energy with respect to the electric field, the $ijkl$ component of the cubic nonlinearity tensor can be written[32]

$$\gamma_{ijkl}(-\omega_\sigma;\omega_1,\omega_2,\omega_3)=\tfrac{1}{6}\hbar^3 P(i,j,k,l;-\omega_\sigma,\omega_1,\omega_2,\omega_3)\times\left(\sum_m\sum_n\sum_p \frac{\langle g|\mu_i|m\rangle\langle m|\overline{\mu_j}|n\rangle\langle n|\overline{\mu_k}|p\rangle\langle p|\mu_l|g\rangle}{(\omega_{mg}-\omega_\sigma-i\Gamma_{mg})(\omega_{ng}-\omega_2-\omega_3-i\Gamma_{ng})(\omega_{pg}-\omega_3-i\Gamma_{pg})} - \sum_m\sum_n \frac{\langle g|\mu_i|m\rangle\langle m|\mu_j|g\rangle\langle g|\mu_k|n\rangle\langle n|\mu_l|g\rangle}{(\omega_{mg}-\omega_\sigma-i\Gamma_{mg})(\omega_{ng}-\omega_2-\omega_3-i\Gamma_{ng})(\omega_{ng}-\omega_3-i\Gamma_{ng})}\right), \quad (1)$$

where $P(i,j,k,l;-\omega_\sigma,\omega_1,\omega_2,\omega_3)$ is a permutation operator defined in such a way that for any permutation of (i,j,k,l), an equivalent permutation of $(-\omega_\sigma,\omega_1,\omega_2,\omega_3)$ is made simultaneously; $\omega_\sigma=\omega_1+\omega_2+\omega_3$ is the polarization response frequency; ω_1, ω_2, and ω_3 indicate the frequencies of the perturbing radiation fields; i, j, k, and l correspond to the molecular axes x,y, and z; m, n, and p denote excited states and g, the ground state; μ_i is the ith component of the dipole operator ($\langle m|\overline{\mu_i}|n\rangle=\langle m|\mu_i|n\rangle-\langle g|\mu_i|g\rangle\delta_{mn}$); ω_{kg} is the excitation frequency from states g to k; and Γ_{mg} is the damping factor of excited state m. We consider that the higher the excited state, the shorter its lifetime,[33] and express the damping, in eV, as[34]

$$\Gamma_{mg}=0.08\times\frac{\omega_{mg}}{\omega_{1g}}. \quad (2)$$

The evolution with the number of excited states included in the SOS formalism of the chain-axis component of the static third-order polarizability, γ_{xxxx}, which totally dominates the cubic response, is displayed in Fig. 3; the main contributions to γ_{xxxx} are collected in Table II. The third-

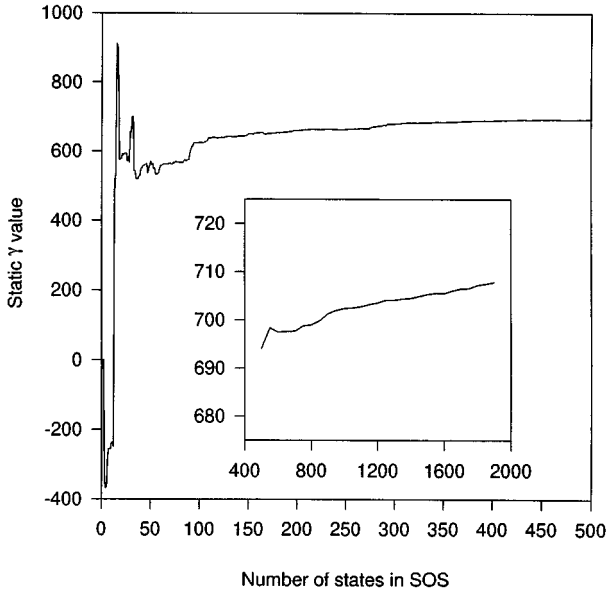

FIG. 3. Evolution of the INDO/MRD-CI/SOS calculated static γ_{xxxx} value according to the basis set size (the inset shows the evolution of γ_{xxxx} from 400 to 1915 states).

order nonlinearity in β-carotene is dominated by the positive channel $1A_g \rightarrow 1B_u \rightarrow m_2A_g \rightarrow 1B_u \rightarrow 1A_g$ and the negative channel $1A_g \rightarrow 1B_u \rightarrow 1A_g \rightarrow 1B_u \rightarrow 1A_g$. Similar results were obtained in polyenes[17–20] as well as in other conjugated oligomers,[35–37] and support the rather successful three-state model, as first proposed by Heflin *et al.*[17] However, as shown in Fig. 3, an accurate (within ~10% error of the converged value) quantitative description of the static cubic polarizability in β-carotene requires us to include at least the 100 lowest excited states in the SOS approach (400 states have to be considered to obtain the fully converged γ_{xxxx} value). Among these states, the $1B_u$, $2A_g$, m_1A_g, m_2A_g, n_1B_u, n_2B_u, and n_3B_u bands (see Table I) play a major role

TABLE II. Main contributions to the chain-axis component γ_{xxxx} of the third-order molecular polarizability of β-carotene, as calculated by the INDO/MRD-CI scheme (purely electronic contributions, computed at the static limit). We also include the sum Σ of all these contributions, as well as the converged γ_{xxxx} value ($\gamma_{xxxx}^{\mathrm{conv}}$), obtained by considering the full set of excited states (1915 states) within the chosen configuration space. All the contributions are given in 10^{-36} esu.

Channel	Contribution
$1A_g \rightarrow 1B_u \rightarrow 1A_g \rightarrow 1B_u \rightarrow 1A_g$	−469
$1A_g \rightarrow 1B_u \rightarrow 2A_g \rightarrow 1B_u \rightarrow 1A_g$	123
$1A_g \rightarrow 1B_u \rightarrow m_1A_g \rightarrow 1B_u \rightarrow 1A_g$	90
$1A_g \rightarrow 1B_u \rightarrow m_2A_g \rightarrow 1B_u \rightarrow 1A_g$	1160
$1A_g \rightarrow 1B_u \rightarrow 2A_g \rightarrow n_1B_u \rightarrow 1A_g$	−49
$1A_g \rightarrow n_1B_u \rightarrow 2A_g \rightarrow 1B_u \rightarrow 1A_g$	−49
$1A_g \rightarrow 1B_u \rightarrow m_2A_g \rightarrow n_1B_u \rightarrow 1A_g$	−59
$1A_g \rightarrow n_1B_u \rightarrow m_2A_g \rightarrow 1B_u \rightarrow 1A_g$	−59
Σ	688
$\gamma_{xxxx}^{\mathrm{conv}}$	708

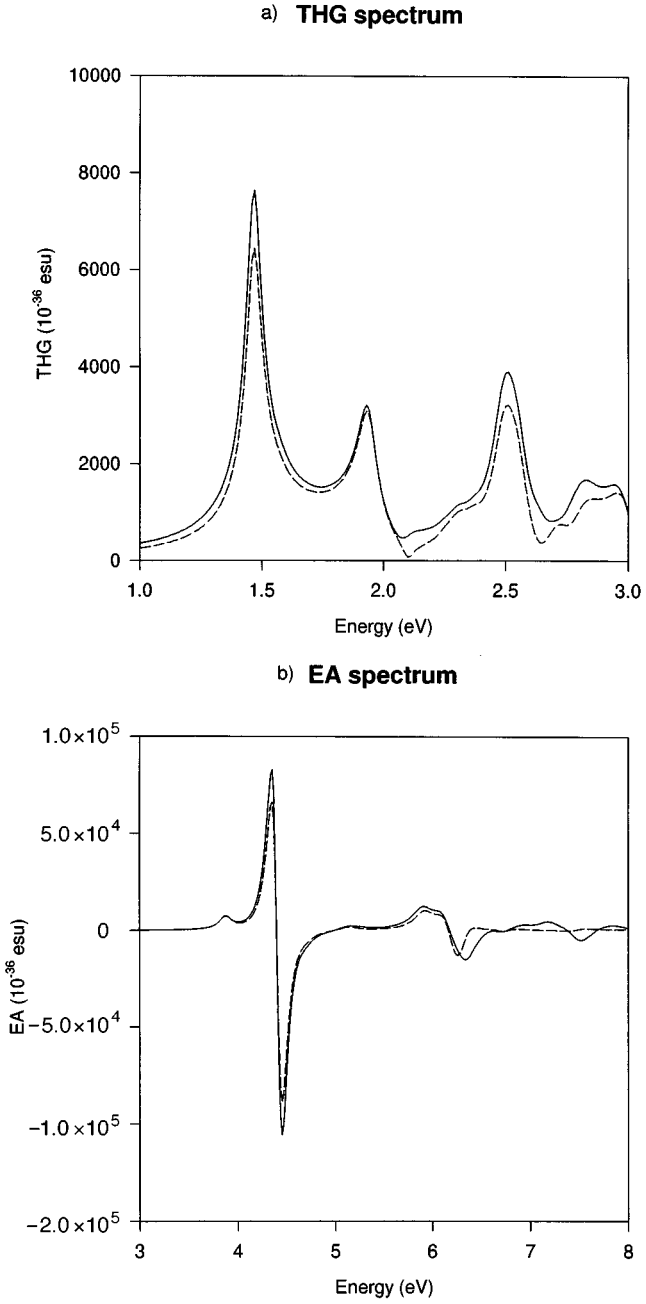

FIG. 4. Comparison between the INDO/MRD-CI/SOS simulations of the third-harmonic generation (THG) spectrum $[|\gamma_{xxxx}(-3\omega;\omega,\omega,\omega)|/5]$ (a) and the electroabsorption spectrum $[\mathrm{Im}(\gamma_{xxxx}(-\omega;\omega,0,0))/5]$ (b), obtained (i) by including the 500 lowest singlet excited states of β-carotene (solid lines); and (ii) by considering the simplified ''eight-state'' model (dashed lines).

in the description of the third-order nonlinearity. It is worth stressing that, within such an ''eight-state'' model ($1A_g$, $1B_u$, $2A_g$, m_1A_g, m_2A_g, n_1B_u, n_2B_u, and n_3B_u), the channels involving the high-lying B_u excited states give rise to negative contributions that reduce the amplitude of the effective response. On the basis of extended Hubbard calculations on polyenes, Guo *et al.* proposed a very convincing general model to describe the microscopic origin of the third-order nonlinearities in conjugated polymers. In this model, developed for infinite chain-length conjugated systems, they include the $1A_g$, $1B_u$, and mA_g states, as well as a higher-

lying B_u state, which possesses a huge transition dipole moment with the mA_g excited state. The high-lying B_u state is involved in pathways giving rise to negative contributions to the total response, and is stated to correspond to the bottom of the conduction band.[38] Their four-state model differs from ours essentially by the fact that the $2A_g$ excited state is not taken into account and by the nature of the couplings involving the high-lying B_u states (as well as the corresponding excitation energies). Such differences could result from finite-size effects, which can certainly not be ignored in the case of the β-carotene molecule.

To calculate the frequency-dependent curves, we apply Eq. (1) for various radiation-field frequencies by considering $\omega_1=\omega_2=\omega_3=\omega$ for the third-harmonic generation (THG) process; and $\omega_1=\omega$ and $\omega_2=\omega_3=0$ for the electroabsorption (EA) spectrum (only the chain-axis component of the nonlinear polarizabilities is retained). In Fig. 4, we show the THG and EA dispersion spectra, as obtained (i) by including the 500 lowest singlet excited states in the SOS formalism, and (ii) on the basis of the simplified ''eight-state'' model defined above. Although small differences are observed in the high-energy domain (above 7 eV) of the electroabsorption spectrum, we find a good agreement between the overall shape of the frequency-dependent nonlinear curves, simulated on the basis of the converged and simplified SOS expressions, which demonstrates the validity of our simplified electronic model.

IV. VIBRONIC STRUCTURE

As proved by our recent investigations on the DANS molecule,[12,13] an important feature when dealing with the study of the dispersion of the optical nonlinearities in conjugated compounds is to include the vibronic structure, i.e., to consider the summation over the vibrational levels of the resonant electronic states. Assuming both the Born-Oppenheimer and Franck-Condon approximations, the total transition dipole moments M_i $(m\rightarrow n;\alpha\rightarrow\beta)$ can be expressed as a product of pure electronic transition moments, $\langle m|\mu_i|n\rangle$, and a nuclear factor corresponding to the overlap between two vibrational wave functions, $F_{mn}^{\alpha\beta}$:

$$M_i(m\rightarrow n;\alpha\rightarrow\beta)=\langle m|\mu_i|n\rangle F_{mn}^{\alpha\beta}, \tag{3}$$

where α (β) denotes the quantum number of vibration in electronic state m (n). If we factorize the vibrational space into $3N$-6 normal modes, denoted ν^x, Eq. (3) becomes

$$M_i(m\rightarrow n;\alpha\rightarrow\beta)=\langle m|\mu_i|n\rangle \prod_{x=1}^{3N-6} \langle \nu_\alpha^x|\nu_\beta^x\rangle. \tag{4}$$

Substitution of Eq. (4) into Eq. (1) leads then to the following expression for the third-order polarizability (we assume that only the zeroth vibrational level of the ground state is populated at room temperature, which is reasonable since the modes coupled to the excitations have energies in the 0.15–0.2-eV range; see below):

$$\gamma_{ijkl}(-\omega_\sigma;\omega_1,\omega_2,\omega_3)=\tfrac{1}{6}\hbar^3 P(i,j,k,l;-\omega_\sigma,\omega_1,\omega_2,\omega_3)$$

$$\times\left(\sum_m\sum_n\sum_p\sum_{(\nu_\beta^x)}\sum_{(\nu_\gamma^x)}\sum_{(\nu_\delta^x)} \frac{\langle g|\mu_i|m\rangle\langle m|\mu_j|n\rangle\langle n|\mu_k|p\rangle\langle p|\mu_l|g\rangle\Pi_{x=1}^{3N-6}\langle 0|\nu_\beta^x\rangle\langle\nu_\beta^x|\nu_\gamma^x\rangle\langle\nu_\gamma^x|\nu_\delta^x\rangle\langle\nu_\delta^x|0\rangle}{(\overline{\omega}_{mg}-\omega_\sigma-i\Gamma)(\overline{\omega}_{ng}-\omega_2-\omega_3-i\Gamma)(\overline{\omega}_{pg}-\omega_3-i\Gamma)}\right.$$

$$\left.-\sum_m\sum_n\sum_{(\nu_\beta^x)}\sum_{(\nu_\gamma^x)} \frac{\langle g|\mu_i|m\rangle\langle m|\mu_j|g\rangle\langle g|\mu_k|n\rangle\langle n|\mu_l|g\rangle\Pi_{x=1}^{3N-6}\langle 0|\nu_\beta^x\rangle^2\langle 0|\nu_\gamma^x\rangle^2}{(\overline{\omega}_{mg}-\omega_\sigma-i\Gamma)(\overline{\omega}_{ng}-\omega_2-\omega_3-i\Gamma)(\overline{\omega}_{pg}-\omega_3-i\Gamma)}\right), \tag{5}$$

where $\Sigma(\nu_\alpha^x)$ corresponds to the sum over the vibrational levels α for each mode x. We stress that these summations are performed *for all intermediate excited states* m, n, *and* p. $\overline{\omega}_{kg}$ denotes the energy difference between states k and g in their respective vibrational level (i.e., the sum of the electronic excitation energy, ω_{kg}, and the difference in vibrational energy between states k and g).

To estimate the overlap functions $\langle\nu_\alpha^x|\nu_\beta^x\rangle$, we adopt the model of the displaced harmonic oscillators. In that model, a harmonic oscillator is associated to each normal mode of vibration in the ground state. Moreover, we assume that the normal modes and hence the vibration frequencies are conserved in the excited states, i.e., we do not take into account possible Duschinski rotation effects.[39] The geometric relaxation in the excited states is simply taken into account by imposing that its potential-energy curve is displaced with respect to that of the ground state. Within this approximation, for displacements a_x and b_x of states m and n, the overlap integral is given by[21]

$$\langle\nu_\alpha^x|\nu_\beta^x\rangle=\frac{e^{-(b_x-a_x)^2/4}}{(2^{\nu_\alpha^x+\nu_\beta^x}\nu_\alpha^x!\,\nu_\beta^x!)^{1/2}} \times\sum_\nu \frac{2^\nu(-1)^{\nu_\beta^x-\nu}(b_x-a_x)^{\nu_\alpha^x+\nu_\beta^x-2\nu}\nu_\alpha^x!\,\nu_\beta^x!}{\nu!(\nu_\alpha^x-\nu)!(\nu_\beta^x-\nu)!}. \tag{6}$$

At this stage, we need to identify the Franck-Condon active vibrations and their displacement parameters. Raman excitation profiles (REP's) offer rich insight into the vibronic detail of an electronic absorption band. In the case of β-carotene, six vibrational normal modes are active in the $1A_g\rightarrow 1B_u$ excitation.[40] Among them, two modes dominate the description of the vibronic structure;[21] the signal-to-noise ratio of the nonlinear experimental data in the spectral range considered does not allow us to check whether the inclusion of other vibrational modes improves the fit. We have thus considered two modes in our model, with a ratio of two

between the associated squared displacements; this ratio was estimated from the REP spectrum (REP intensities can be shown to be proportional to the square of the potential displacements[41]). In the case of the $1A_g \rightarrow 1B_u$ transition, the absolute value of the displacements are obtained from a fit of the linear absorption spectrum.

For the other excited states ($2A_g$, m_1A_g, m_2A_g, n_1B_u, n_2B_u, and n_3B_u), the Franck-Condon active vibrations and corresponding displacements are unknown and we are thus forced to make the following severe assumptions.

(i) The INDO/MRD-CI π-bond orders in the excited states of β-carotene indicate that much stronger lattice distortions occur in the $2A_g$ excited state with respect to the other excited states included in the simplified model. These results are confirmed by experimental data, indicating much larger bond-length modifications in the lowest two-photon excited state of octatetraene with respect to the lowest one-photon excited state.[42,43] We thus considered larger values for the displacement parameters in the $2A_g$ excited state, which are consistent with earlier investigation of the THG dispersion curve of β-carotene.[21]

(ii) We chose the same set of displacement parameters for the m_1A_g, m_2A_g, n_1B_u, n_2B_u, and n_3B_u states as for the $1B_u$. This assumption leads indeed to a significant simplification of Eq. (4), since only the terms conserving the same number of vibrational quanta are allowed between states with equivalent geometric structures. Moreover, it provides frequency-dependent nonlinear curves that are in good agreement with experiment (see Sec. V). To check more closely on the validity of this approximation, a high-level description of the potential-energy curves of these excited states is required, which is unfortunately out of our reach for a molecule like β-carotene.

V. LINEAR AND NONLINEAR FREQUENCY-DEPENDENT CURVES OF β-CAROTENE

In Figs. 5, 6, 7, and 8, we present, respectively, the one-photon optical absorption (OPA), the amplitude of the third-harmonic generation process, the phase of the THG process, and the electroabsorption spectra of β-carotene, as calculated on the basis of the simplified ''eight-state'' model discussed above. Before going into the description of the linear and nonlinear spectra, we would like to make the following comments concerning the quality of the description of the excited states afforded by the INDO/MRD-CI technique. To allow for a direct comparison to the experimental data, we were forced to shift all the excited states by 1.93 eV. Such a large difference between the measured and calculated excitation energies is mainly the consequence of an unbalanced description of the correlation effects in the ground state and in the excited states, due to the fact that we include more double excitations in the CI calculation than higher-order excitations; this leads to an overstabilization of the ground state with respect to all excited states. However, we found it essential in the CI wave functions to take into account as many as possible doubly excited configurations in order to reproduce the ordering of the lowest two excited states correctly; using our MRD-CI formalism, we calculate the relaxed $2A_g$ excited state at about 0.5 eV below the zero-phonon level of the $1B_u$ excited state, which is in good

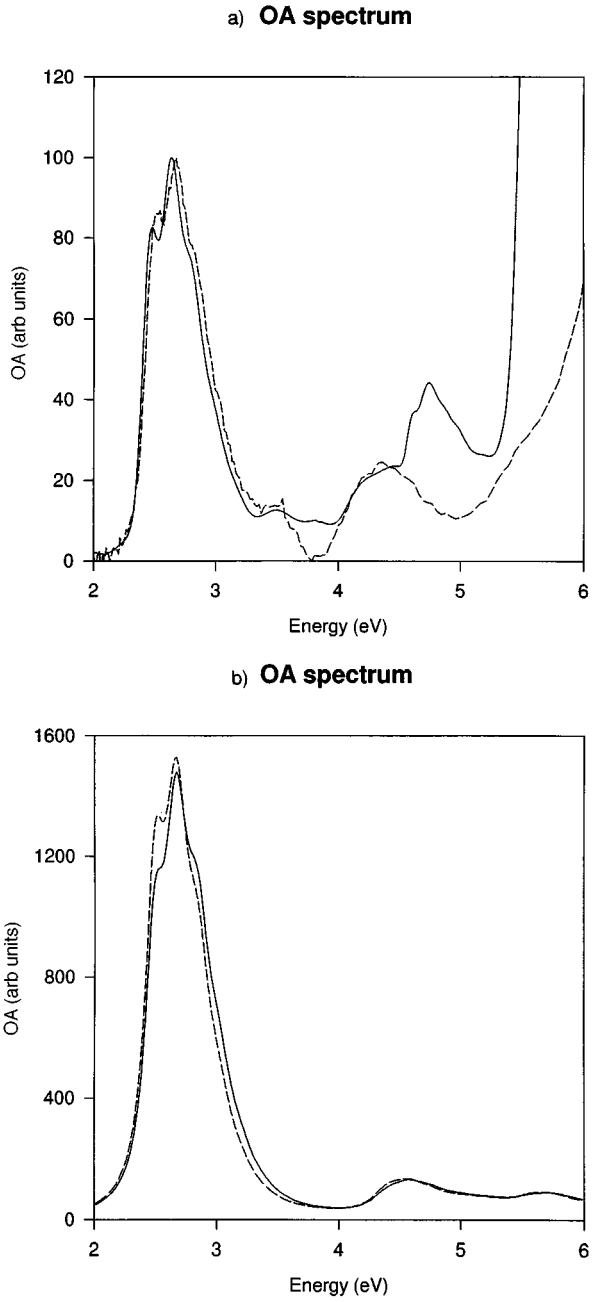

FIG. 5. Linear optical-absorption spectrum of β-carotene (a) as measured experimentally (sample 1: solid line; sample 2: dashed line); and (b) as simulated at the INDO/MRD-CI/SOS level ($\mathrm{Im}\langle\alpha(-\omega;\omega)\rangle$) (the solid line corresponds to the first series of displacements, b_v^1 in Table III; the dashed line corresponds to the second set, b_v^2).

agreement with the values extracted from various optical measurements, ranging from 0.33 eV (Ref. 44) to 0.63 eV,[45] and the energy (0.67 eV) extrapolated from one- and two-photon absorption data on polyenes.[21] A slightly larger energy separation (0.76 eV) is deduced from the electroabsorption measurements presented in this work.

Excited-state absorption spectra of long carotenoids were reported recently.[46] These transient measurements show a strong $S_1 \rightarrow S_n$ absorption, that correspond to the $2A_g \rightarrow n_1B_u$ excitation in our calculations. For β-carotene, the experimental data give rise to a singlet-singlet 0-0 transition energy that

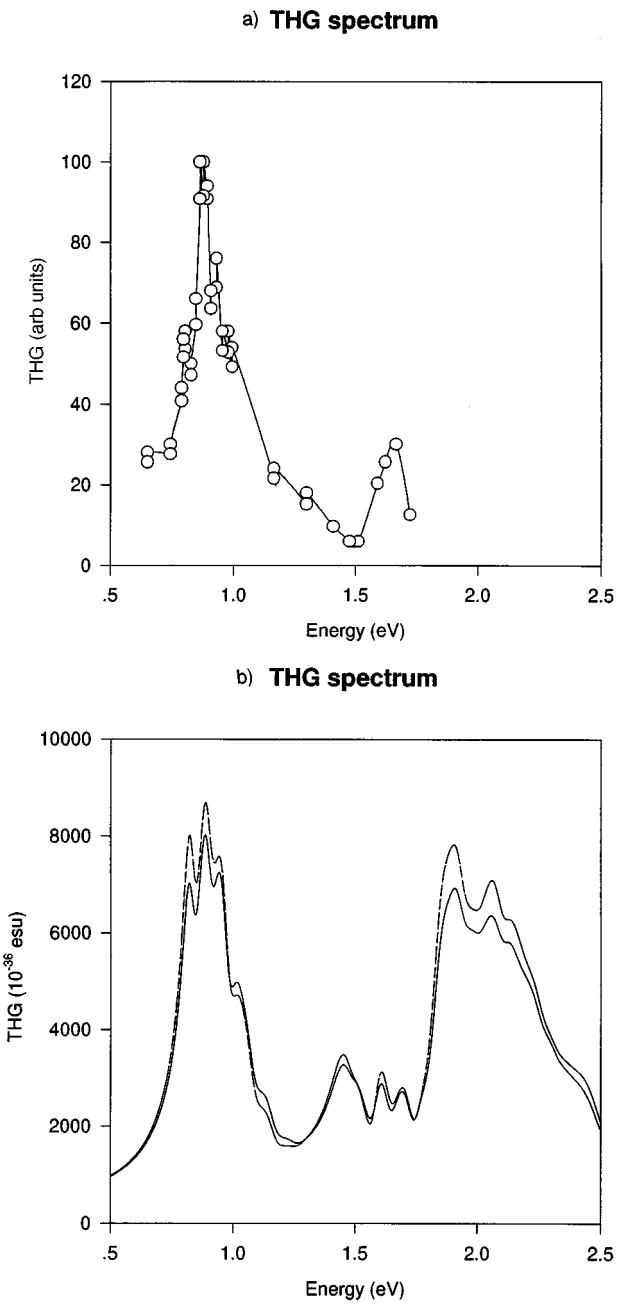

FIG. 6. Third-harmonic-generation amplitude spectrum of β-carotene (a) as measured experimentally (circles; the line is a guide to the eye); and (b) as simulated at the INDO/MRD-CI/SOS level [$|\gamma_{xxxx}(-3\omega;\omega,\omega,\omega)|/5$] (the solid line corresponds to the first series of displacements, b_v^1 in Table III; the dashed line corresponds to the second set, b_v^2).

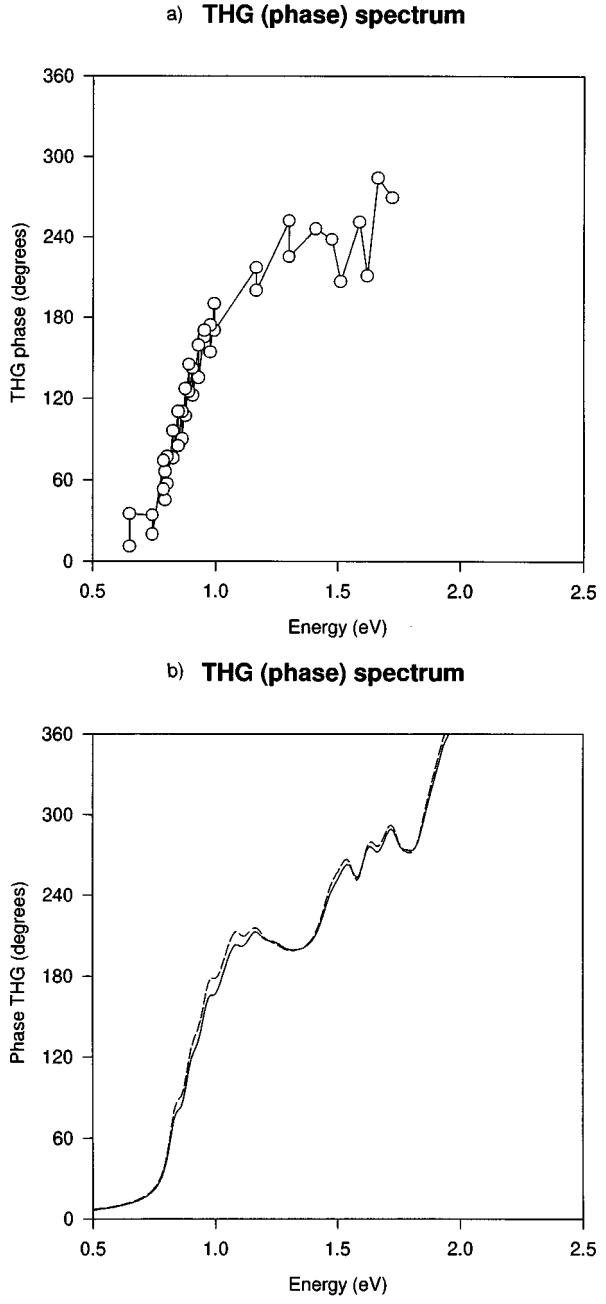

FIG. 7. Third-harmonic-generation phase spectrum of β-carotene (a) as measured experimentally (circles; the line is a guide to the eye); and (b) as simulated at the INDO/MRD-CI/SOS level (the solid line corresponds to the first series of displacements, b_v^1 in Table III; the dashed line corresponds to the second set, b_v^2).

amounts to ~2.8 eV, in reasonable agreement with the calculated ~2.4-eV value. Furthermore, the INDO/MRD-CI $1A_g \rightarrow 1B_u$ transition dipole moment (~14 D) compares very well with the value extracted from the linear absorption spectrum of a β-carotene-doped polystyrene thin film (~13.5 D).[15] We are thus confident that the MRD-CI scheme provides both good estimates of the energy separations between the excited states as well as accurate wave functions (from which the transition dipole moments are computed).

The main absorption band of β-carotene, with an onset at ~2.3 eV and a maximum peak at ~2.67 eV, is assigned to the $1A_g \rightarrow 1B_u$ electronic excitation, characterized by a very large transition dipole moment. The vibronic structure, clearly observed in the experimental data, is well described by our theoretical model including two normal modes of vibration (Fig. 5); the good agreement between the experimental and theoretical line shapes shows that it is sufficient to consider only two vibrational modes in our theoretical modeling. Differences in the shape of the $1B_u$ absorption band are observed between samples 1 and 2, and are associated with a different degree of order in the two samples; these can be accounted for by considering two series of displacement parameters, as indicated in Table III. Weak ab-

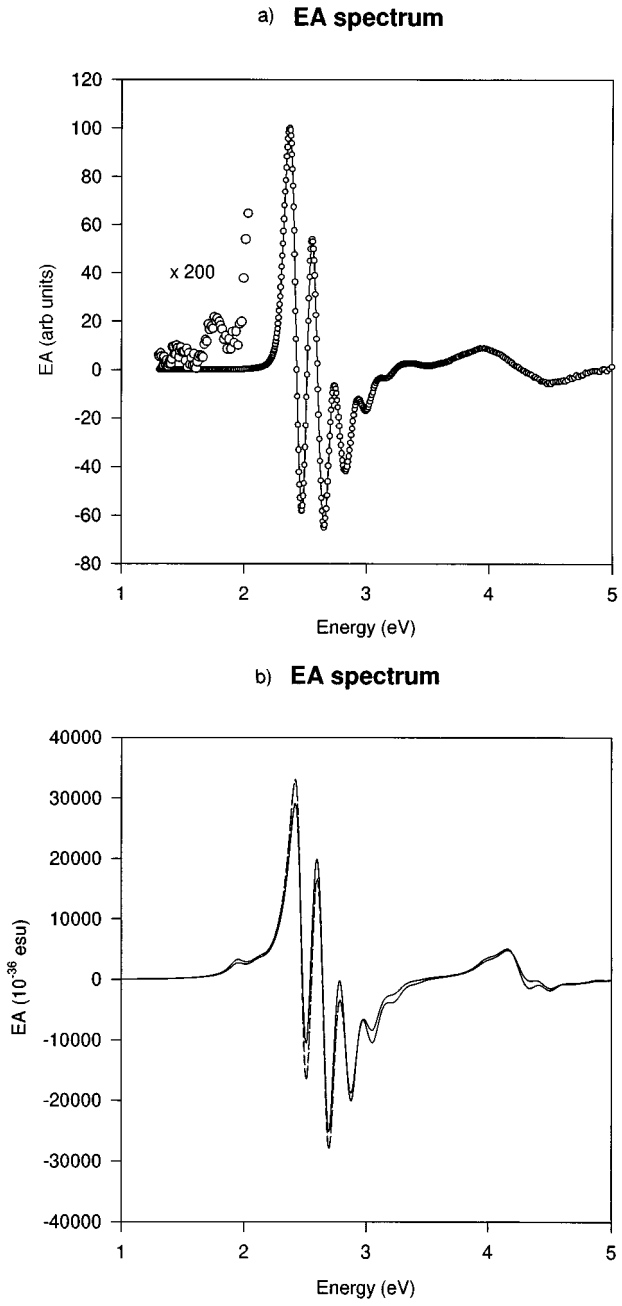

FIG. 8. Electroabsorption spectrum of β-carotene (a) as measured experimentally (circles; the line is a guide to the eye); and (b) as simulated at the INDO/MRD-CI/SOS level $[\mathrm{Im}(\gamma_{xxxx}(-\omega;\omega,0,0))/5]$ (the solid line corresponds to the first series of displacements, b_v^1 in Table III; the dashed line corresponds to the second set, b_v^2). Note that we also show a magnification (by a factor 200) of the experimental spectrum between 1.2 and 2.1 eV to see the $2A_g$ resonance feature.

sorption peaks are also observed at higher energy. The peak at 3.56 eV on the experimental spectrum is referred to as a ''cis-peak'' on account of its intensification following the introduction of cis linkages into the polyene chain.[16] The broad absorption band extending from 4 to 5 eV involves contributions of several excited states including the n_1B_u states involved in our minimal model as well as other excited states, described in terms of single excitations from molecular levels with large weights on the cyclohexene external rings. As these are mainly polarized in the direction perpendicular to the chain axis, they only contribute weakly to the nonlinear response (totally dominated by the chain-axis component) and, therefore, are not considered in our model to describe the cubic nonlinearities. Note also that local residual absorption of polystyrene is observed at 4.75 eV in the optical-absorption spectrum measured for sample 1. A more in-depth analysis of the linear response will be presented elsewhere.[47]

TABLE III. Parameters considered in the displaced oscillator model for the description of the vibronic couplings. x is a vibrational mode with frequency ν_x and displacement b_x^1 or b_x^2. The vibrational frequencies are taken from resonance Raman spectra (Ref. 37). The displacement parameters for the $1B_u$ excited state were adjusted in order to reproduce the experimental data for samples 1 and 2 and were assumed to be the same for the m_1A_g, m_2A_g, n_1B_u, n_2B_u, and n_3B_u states; larger displacements were considered for the $2A_g$ excited state, to account for the more pronounced geometric deformations taking place in that state (see text).

	$2A_g$	$1B_u$, m_1A_g, m_2A_g, n_1B_u, n_2B_u, and n_3B_u
$h\nu_x$ (eV)	0.189	0.189
$h\nu_x'$ (eV)	0.143	0.143
b_x^1/b_x^2	1.83/1.66	1.29/1.18
$b_{x'}^1/b_{x'}^2$	1.30/1.17	0.92/0.83

The theoretical frequency-dependent THG spectrum of β-carotene (Fig. 6) shows resonances associated with the different excited states involved in the minimal model: (i) the low-lying feature, peaking at ~0.9 eV, corresponds to the overlapping resonances to the $1B_u$ and $2A_g$ singlet excited states; (ii) the peak at ~1.5 eV is a three-photon resonance associated with the n_1B_u state, which is characterized by large transition dipole moments with both the $2A_g$ and m_2A_g excited states; (iii) the features located at ~1.6 and ~1.7 eV result, respectively, from two- and three-photon resonances to the coupled m_1A_g and n_2B_u excited states; and (iv) the intense resonant peak at ~2 eV is due to superimposed resonances to the coupled m_2A_g and n_3B_u states. Note that the relative intensity of these peaks is very sensitive to the exact location of the different excited states, since most of them involve double-resonance phenomena (compare the shape of the THG curves in Figs. 4 and 6). McWilliams and Soos calculated similar double resonances in polyenes, and showed that their intensity is strongly reduced by including interchain interactions that modify the energy separation between the A_g and B_u states involved in the overlapping resonances.[48] Guo and Mazumdar argued that double resonances are due to finite-size effects, and should disappear in polymers.[49] Another possibility that was investigated by Soos and Mukhopadhyay[21] is related to the relative sign of the displacements, b, associated to the coupled excited states; considering b values with opposite signs leads to a much weaker resonance, since the vibrational overlap between the two states is much smaller in this case. Clearly, this point remains unsolved and requires more work (that is, it would be interesting to extend the THG measurements up to 2 eV, to check whether such double-resonance effects actually occur around that energy value).

Nevertheless, in the energy domain covered by the experimental data, we find an overall good agreement between the measured and calculated shapes of the THG curve (the calculated second resonant peak, however, is redshifted by ~0.2 eV with respect to the corresponding measured feature). A quantitative comparison between the experimental and theoretical γ values should be considered with caution: on one hand, the measured values are always affected by dispersion effects, that are very sensitive to the displacement and damping factors adopted in the model; and on the other hand, due to the different approximations considered in the INDO/MRD-CI scheme, this technique only provides reasonable estimates for the absolute values of the third-order polarizabilities.[30] For illustration, the chain-axis component value of γ, estimated from the calculated THG curve in Fig. 6, ranges from 7.5×10^{-33} to 12.0×10^{-33} esu in the energy range from ~0.6 to ~0.7 eV, while the measured value at 0.66 eV is 8×10^{-33} esu.[50]

As first pointed out by Soos and Mukhopadhyay,[21] the low-energy part of the frequency-dependent THG curve is very well reproduced by a model including the $2A_g$ excited state, which, in contrast to the model of Guo *et al.*,[38] makes a nonvanishing contribution to the third-order response. The INDO/MRD-CI/SOS simulated THG spectrum also compares well with the experimental spectrum of van Beek *et al.*,[15] although our ''eight-state'' model is significantly different from their three-state model. From the fit of the experimental THG data, they obtained a $1B_u\rightarrow mA_g$ transition dipole moment of ~31D (i.e., 2.3 times the $1A_g\rightarrow1B_u$ transition dipole), with the dominant mA_g state lying ~0.3 eV above the $1B_u$ (i.e., 1.1 times the $1B_u$ excitation energy). This description is in marked contrast with that obtained on the basis of exact semiempirical Pariser-Parr-Pople (PPP) (Refs. 17–20 and 47) or highly correlated *ab initio* (Ref. 30) calculations in short polyenes (where the ratio between the $1B_u\rightarrow mA_g$ and $1A_g\rightarrow1B_u$ transition dipole moments and between the mA_g and $1B_u$ excited-state energies are both close to 1.5–1.7). This feature clearly points out that the three-state model is inadequate to describe the third-order nonlinear response of finite conjugated chains. Moreover, we note that neglecting the $2A_g$ excited state would lead to a much more intense peak at ~1.5 eV, since, in this frequency range, the γ value is determined by the competition between positive and negative channels involving the lowest two-photon excited state, i.e., mainly $1A_g\rightarrow1B_u\rightarrow2A_g\rightarrow1B_u\rightarrow1A_g$ (positive contribution) and $1A_g\rightarrow1B_u\rightarrow2A_g\rightarrow n_1B_u\rightarrow1A_g$ (negative contribution).

The balanced description of both types of contributions also allows for a proper description of the phase of the third-harmonic generation response; see Fig. 7. In the energy range covered by the experiments, both the measured and calculated frequency-dependent curves of the THG phase are characterized by three domains: (i) between 0.5 and 1.0 eV, the phase increases from 0° to 180° (as a consequence of the three-photon resonance to the $1B_u$ state); (ii) a plateau is reached between 1.1 and 1.4 eV, where the phase fluctuates around 200°; and (iii) the second resonance feature (three-photon resonance to the n_1B_u state) leads to the appearance of a step in the frequency-dependent phase spectrum just above 1.5 eV.

The optical response associated with electroabsorption, as

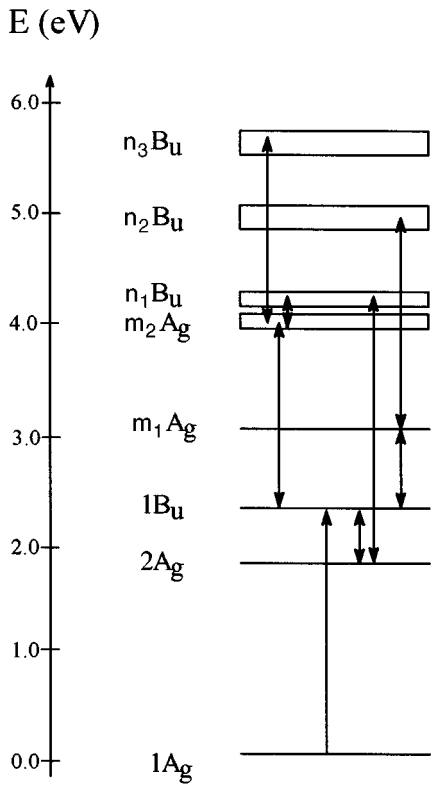

FIG. 9. Energy diagram of the ''eight-state'' model for β-carotene. We also indicate the main couplings, through large transition dipole moments, among the electronic states of the molecule (arrows).

is the case for typical linear optical absorption, is resonantly enhanced when the perturbing radiation-field frequency is close to the energy of one of the excited states of the system; therefore, except for very close-lying excited states, double resonances to coupled A_g and B_u states are avoided for the electroabsorption spectrum, which provides a more meaningful test for the theoretical models. Moreover, since the applied static electric field breaks the molecular symmetry, both A_g and B_u excited states can be accessed by this technique. In the case of β-carotene (Fig. 8), besides the well-resolved resonance to the $1B_u$ excited state, characterized by oscillations resulting from the vibronic progression, we calculate (i) a very weak feature at lower energy, that we associate with the low-lying $2A_g$ excited state; (ii) a broad positive peak around 4 eV; and (iii) a negative feature just above (centered around 4.3 eV) corresponding to superimposed absorptions into the two-photon m_2A_g and the higher-lying n_1B_u bands. We stress that, from our theoretical approach, we cannot distinguish the contributions associated with the m_2A_g and n_1B_u bands in the high-energy region of the EA spectrum, since the NLO response in that frequency domain is dominated by channels where these states are strongly coupled (of the form $1A_g\rightarrow1B_u\rightarrow m_2A_g\rightarrow n_1B_u\rightarrow1A_g$).

The theoretical simulation of the electroabsorption spectrum between 2 and 6 eV is in excellent agreement with the experimental spectrum, which confirms the accuracy of our model to describe the dynamic NLO response of β-carotene. The redshift of the $1B_u$ transition observed in the experimental EA spectrum can be explained within the theoretical

model by the larger coupling of the $1B_u$ excited state to the higher-lying m_2A_g state with respect to the ground state (the effects of the $2A_g$ and m_1A_g excited states on the position of the $1B_u$ excitation more or less cancel each other). Note also that, in accord to the theoretical predictions, a weak electroabsorption signal associated with the $2A_g$ excited state is observed just below 2 eV. The small intensity associated with this peak (despite the rather large $1B_u$-$2A_g$ coupling) is due to the superimposition of the various contributions described above, and can only be reproduced by considering both the $2A_g$ and n_1B_u states, in contrast to the previous models proposed by Soos and Mukhopadhyay[21] and van Beek *et al.*[15]

VI. SYNOPSIS

On the basis of extended configuration-interaction calculations, we investigated the nature of the essential states contributing primarily to the nonlinear optical third-order response of the β-carotene molecule. The cubic nonlinearity is dominated by eight states or ''bands'' of states (see Fig. 9): (1) the ground state, $1A_g$; (2) the lowest two-photon excited state, $2A_g$; (3) the lowest one-photon excited state, $1B_u$; (4) and (5) two bands of two-photon states, m_1A_g and m_2A_g, possessing large transition dipole moments with the $1B_u$ state; and (6), (7), and (8), three bands of one-photon states, n_1B_u, n_2B_u, and n_3B_u, coupled to the $2A_g$, m_1A_g, and m_2A_g states, respectively.

We applied the ''eight-state'' model to the simulation of the dispersion curves of two third-order processes: third-harmonic generation and electroabsorption; the vibronic structure of the spectra was described by including Franck-Condon factors within the displaced oscillators approximation. For both processes, the theoretical curves are in good agreement with the experimental data, which supports the validity of our model. Moreover, a very similar model was successfully applied to calculate the third-harmonic generation and two-photon absorption spectra in heptathiophene.[36] Although further work is required, we are confident that our model also holds true for other conjugated systems. In comparison to previous works,[19,21,38] the information provided by this study can be summarized in two points: (i) the $2A_g$ excited state makes a nonvanishing contribution to the third-order response (at least for finite chains); and (ii) each relevant two-photon state, coupled to the $1B_u$ state, also possesses large dipole moments with higher-lying B_u excited states, that therefore need to be included in the SOS expression for a proper description of the dynamic NLO response.

ACKNOWLEDGMENTS

We wish to thank Professor Z. G. Soos for very stimulating discussions. The Mons-Sheffield collaboration is supported by the Human Capital and Mobility Network ''Novel Third-Order NLO Molecular Materials.'' The work in Mons was also partly supported by the Belgian Government ''Services Fédéraux des Affaires Scientifiques, Techniques et Culturelles'' (''Pôle d'Attraction Interuniversitaire No. 16: Chimie Supramoléculaire et Catalyse''), FNRS/FRFC, and an IBM Academic Joint Study. J.C. and D.B. acknowledge support from Belgian National Fund for Scientific Research (FNRS).

*Current address: Department of Physics, Washington State University, Pullman, Washington 99164.

[1] *Nonlinear Optical Effects in Organic Polymers*, Vol. 162 of *NATO Advanced Study Institute, Series E: Applied Sciences*, edited by J. Messier, F. Kajzar, P. Prasad, and D. Ulrich (Kluwer, Dordrecht, 1989); *Nonlinear Optical Properties of Organic Molecules and Crystals*, edited by D. S. Chemla and J. Zyss (Academic, Orlando, 1987); *Conjugated Polymeric Materials: Opportunities in Electronics, Optoelectronics, and Molecular Electronics*, Vol. 182 of *NATO Advanced Study Institute, Series E: Applied Sciences*, edited by J. L. Brédas and R. R. Chance (Kluwer, Dordrecht, 1990), Vol. 182.

[2] B. Lawrence, W. E. Torruellas, M. Cha, M. L. Sundheimer, G. I. Stegeman, J. Meth, S. Etemad, and G. Baker, Phys. Rev. Lett. **73**, 597 (1994); B. L. Lawrence, M. Cha, W. E. Torruellas, G. I. Stegeman, S. Etemad, G. Baker, and F. Kajzar, Appl. Phys. Lett. **64**, 2773 (1994).

[3] R. R. Chance, M. L. Shand, C. Hogg, and R. Silbey, Phys. Rev. B **22**, 3540 (1980).

[4] T. Hasegawa, K. Ishikawa, T. Kanetake, T. Koda, K. Takeda, H. Kobayashi, and K. Kudobera, Chem. Phys. Lett. **171**, 239 (1990); M. Yoshizawa, Y. Hattori, and T. Kobayashi, Phys. Rev. B **49**, 14 085 (1994).

[5] P. A. Gass, I. Abram, R. Ray, and M. Schott, J. Chem. Phys. **100**, 88 (1994).

[6] F. Kajzar, S. Etemad, G. L. Baker, and J. Messier, Solid State Commun. **63**, 1113 (1987).

[7] T. W. Hagler and A. J. Heeger, Phys. Rev. B **49**, 7313 (1994).

[8] G. S. W. Graig, R. E. Cohen, R. R. Schrock, A. Esser, and W. Schrof, Macromolecules **28**, 2512 (1995).

[9] W. E. Torruellas, D. Neher, R. Zanoni, G. I. Stegeman, F. Kajzar, and M. Leclerc, Chem. Phys. Lett. **175**, 11 (1990); M. Cha, W. E. Torruellas, S. H. Yuan, G. I. Stegeman, and M. Leclerc, J. Opt. Soc. Am. B **12**, 882 (1995).

[10] F. Kajzar, G. Ruani, C. Taliani, and R. Zamboni, Synth. Met. **37**, 1178 (1990).

[11] T. Sugiyama, T. Wada, and H. Sasabe, Synth. Met. **28**, 323 (1989).

[12] W. E. Torruellas, R. Zanoni, G. I. Stegeman, G. R. Möhlmann, E. W. P. Erdhuisen, and W. H. G. Horsthuis, J. Chem. Phys. **94**, 6851 (1991); M. Cha, W. E. Torruellas, G. I. Stegeman, W. H. G. Horsthuis, G. R. Möhlmann, and J. Meth, Appl. Phys. Lett. **65**, 2648 (1994).

[13] D. Beljonne, J. L. Brédas, M. Cha, W. E. Torruellas, G. I. Stegeman, J. W. Hofstraat, W. H. G. Horsthuis, and G. R. Möhlmann, J. Chem. Phys. **103**, 7834 (1995).

[14] S. Aramaki, W. E. Torruellas, R. Zanoni, and G. I. Stegeman, Opt. Commun. **85**, 527 (1991).

[15] J. B. van Beek, F. Kajzar, and A. C. Albrecht, J. Chem. Phys. **95**, 6400 (1991); J. B. van Beek and A. C. Albrecht, Chem. Phys. Lett. **187**, 269 (1991).

[16] F. Rohlfing, D. D. C. Bradley, A. Eberhardt, K. Müllen, J. Cornil, D. Beljonne, and J. L. Brédas, Synth. Met. **76**, 35 (1996).

[17] J. R. Heflin, K. Y. Wong, O. Zamani-Khamiri, and A. F. Garito, Phys. Rev. B **38**, 1573 (1988).

[18] B. M. Pierce, J. Chem. Phys. **91**, 791 (1989).

[19] P. C. M. McWilliams, G. W. Hayden, and Z. G. Soos, Phys. Rev. B **43**, 9777 (1991).
[20] Z. Shuai, D. Beljonne, and J. L. Brédas, J. Chem. Phys. **97**, 1132 (1992).
[21] Z. G. Soos and D. Mukhopadhyay, J. Chem. Phys. **101**, 5515 (1994).
[22] V. Ricci, Ph.D. thesis (University of Central Florida), 1995.
[23] M. J. S. Dewar, E. G. Zoebisch, E. F. Healy, and J. J. P. Stewart, J. Am. Chem. Soc. **107**, 3902 (1985).
[24] E. Ehrenfreund, D. Moses, A. J. Heeger, J. Cornil, and J. L. Brédas, Chem. Phys. Lett. **196**, 84 (1992).
[25] J. Ridley and M. Zerner, Theor. Chim. Acta **32**, 111 (1973).
[26] R. J. Buenker and S. D. Peyerimhoff, Theor. Chim. Acta **35**, 33 (1974).
[27] P. Tavan and K. Schulten, J. Chem. Phys. **85**, 6602 (1987); Phys. Rev. B **36**, 4337 (1987).
[28] N. Mataga and K. Nishimoto, Z. Phys. Chem. **13**, 140 (1957).
[29] K. Ohno, Theor. Chim. Acta **2**, 219 (1964).
[30] D. Beljonne, L. Serrano-Andrès, B. Roos, and J. L. Brédas (unpublished).
[31] B. J. Orr and J. F. Ward, Mol. Phys. **20**, 513 (1971).
[32] A. Wiletts, J. E. Rice, D. M. Burland, and D. P. Shelton, J. Chem. Phys. **97**, 7590 (1992).
[33] We assume that the damping factor Γ_{mg} can be substituted for by the longitudinal rate constant Γ_{mm}, that is inversely proportional to the excited-state lifetime; see Y. R. Shen, in *Nonlinear Spectroscopy*, edited by N. Bloembergen (North-Holland, Amsterdam, 1977), pp. 277–281.
[34] Z. Shuai and J. L. Brédas, Phys. Rev. B **44**, 5962 (1991).
[35] D. Beljonne, Z. Shuai, and J. L. Brédas, J. Chem. Phys. **98**, 8819 (1993).
[36] D. Beljonne and J. L. Brédas, J. Opt. Soc. Am. B **11**, 1380 (1994).
[37] D. Beljonne and J. L. Brédas, Phys. Rev. B **50**, 2841 (1994).
[38] D. Guo, S. Mazumdar, S. N. Dixit, F. Kajzar, F. Jarka, Y. Kawabe, and N. Peyghambrian, Phys. Rev. B **48**, 1433 (1993).
[39] F. Duschinski, Acta Physiochim. USSR **1**, 551 (1937).
[40] A. R. Mantini, M. P. Marzocchi, and G. Smulevich, J. Chem. Phys. **91**, 95 (1989).
[41] W. Siebrand and M. Z. Zgierski, J. Chem. Phys. **71**, 3561 (1979); B. R. Stallard, P. M. Champion, P. R. Callis, and A. C. Albrecht, *ibid.* **78**, 712 (1983).
[42] B. E. Kohler, C. Spangler, and C. Westerfield, J. Chem. Phys. **89**, 5422 (1988).
[43] I. W. Sztainbuch and G. E. Leroi, J. Chem. Phys. **93**, 4642 (1990).
[44] R. J. Trash, H. L. B. Fong, and G. E. Leroi, J. Chem. Phys. **67**, 5930 (1977).
[45] K. Gaier, A. Angerhofer, and H. C. Wolf, Chem. Phys. Lett. **187**, 103 (1991).
[46] P. O. Andersson and T. Gillbro, J. Chem. Phys. **103**, 2509 (1995).
[47] F. Rohlfing, D. D. C. Bradley, A. Eberhardt, K. Müllen, J. Cornil, D. Beljonne, and J. L. Brédas (unpublished).
[48] P. C. M. McWilliams and Z. G. Soos, J. Chem. Phys. **95**, 2127 (1991).
[49] D. Guo and S. Mazumdar, J. Chem. Phys. **97**, 2170 (1992).
[50] J. P. Hermann, D. Ricard, and J. Ducuing, Appl. Phys. Lett. **23**, 178 (1973).